

Experimental observation of resonant filtering in a two-dimensional phononic crystal waveguide

Jerôme O. Vasseur^{*,I}, Pierre A. Deymier^{II}, Maxime Beaugeois^{III}, Yan Pennec^{I,IV}, Bahram Djafari-Rouhani^I and Dominique Prevost^I

^I Laboratoire de Dynamique et Structures des Matériaux Moléculaires, UMR CNRS 8024, UFR de Physique, Université de Lille I, 59655 Villeneuve d'Ascq Cédex, France

^{II} Department of Materials Science and Engineering, University of Arizona, Tucson, Arizona 85721, USA

^{III} Laboratoire de Physique des Lasers, Atomes et Molécules, UMR CNRS 8523, UFR de Physique, Université de Lille I, 59655 Villeneuve d'Ascq Cédex, France

^{IV} Laboratoire de Structure et Propriétés de l'Etat Solide, UMR CNRS 8008, UFR de Physique, Université de Lille I, 59655 Villeneuve d'Ascq Cédex, France

Received June 30, 2004; accepted September 28, 2004

Phononic crystal / Waveguide / Resonator / Filtering

Abstract. Transmission of acoustic waves through a two-dimensional composite material made of PVC cylinders surrounded by air is measured experimentally. The spectrum presents a very large absolute band gap in the audible frequency range. A waveguide created inside this phononic crystal by removing a row of cylinders can transmit very efficiently the waves falling inside the stop band. We show the existence of deaf modes in the band structure of the linear waveguide. Resonant filtering is also demonstrated experimentally by coupling the waveguide to a side branch resonator of variable length. Frequency filtering is observed in the form of narrow dips in the transmission spectrum of the waveguide. Most of these observations compare favorably with theoretical calculations of dispersion curves and transmission coefficients of model structures using the plane wave expansion and the finite difference time domain methods. Narrow dips similar to those of the guide with resonator are also observed in the transmission spectrum of a waveguide with a sharp bend.

1. Introduction

Acoustic band gap (ABG) materials, are inhomogeneous materials made of two- or three-dimensional repetitive arrangements of inclusions in a matrix constituted of a different substance [1–3]. ABG materials, also called phononic crystals, possess absolute stop bands in their acoustic transmission spectrum (i.e. gaps independent of the direction of propagation of an incident wave). The removal of inclusions along some pathway in the phononic crystal produces acoustic waveguides [4–9]. Acoustic waves that would not propagate otherwise in a phononic crystal can be guided with minimal loss along such waveguides. Low

loss transmission can be achieved in linear waveguides as well as guides with sharp bends. Furthermore, the passing band of a guide can be altered by attaching resonators to its side. For instance, side branch resonators obtained by removing additional inclusions in a direction perpendicular to a linear waveguide in a two-dimensional phononic crystal, induce zeros of transmission in the spectrum of the unperturbed guide [4, 7]. The zeros of transmission appear as narrow dips with frequencies depending on the geometry of the resonator. Such resonant filters rejecting specific frequencies may serve as building elements for the design of specific functions in the treatment of acoustic signals.

The existence of absolute stop bands in phononic crystals was demonstrated experimentally [10–12], several years after their theoretical prediction [1–3]. Experimental observation of a phononic crystal waveguide was reported only recently [13, 14] following several numerical studies of similar guides [4–7]. In support of a recent theoretical study showing the existence and properties of resonant filters in two-dimensional phononic crystal waveguides [4], this paper shows experimentally that the presence of resonators in the vicinity of a waveguide induces narrow zeros of transmission in the passing band of the guide. The experimental results are supplemented by numerical calculations of dispersion curves and transmission coefficients based on the plane wave expansion (PWE) and the finite difference time domain (FDTD) methods.

This paper is organized as follows. In Section 2, we present with some details the experimental structures and setup used to measure acoustic transmission spectra. The numerical methods employed to support the experiments are also reviewed in that section. Section 3 contains the results. These consist essentially of measured and calculated transmission spectra for several structures, namely a perfect phononic crystal, a linear waveguide in a phononic crystal, a linear waveguide with a side branch resonator of variable length and a bent waveguide. Finally, some conclusions are drawn in Section 4.

* Correspondence author (e-mail: jerome.vasseur@univ-lille1.fr)

2. Systems and methods

2.1 Systems

The basic experimental system is a two-dimensional solid/fluid phononic crystal composed of 18×18 Polyvinyl Chloride (PVC) cylinders in air. The cylinders are one meter long, parallel to the Z direction of the (O, X, Y, Z) Cartesian coordinates system (see inset in Fig. 1) and are arranged on a square array with lattice parameter $a = 2.7$ cm (see illustration in Fig. 1a). The cylinder radius is $r = 1.29$ cm. This results in a filling factor, $f = \pi r^2/a^2 = 0.717$. We have chosen a PVC/air phononic crystal with lattice parameter in the centimeter range to achieve acoustic band gaps in the audible range of frequency [1–3]. Acoustic waveguides and resonators are easily created in this structure by removing cylinders. More specifically, we have constructed, a linear waveguide (Fig. 1b), two resonators of different lengths coupled to a linear guide (Figs. 1c and 1d) and a guide with a sharp bend (Fig. 1e).

2.2 Methods

2.2.1 Experiments

We measure the transmission across the phononic crystal and along the guides with a speaker connected to a function generator (HP3324A) and a microphone whose frequency response lies in the range [40 Hz–12 kHz]. The speaker produces the incoming signal and the microphone records the transmitted one. The transmitted signal is detected with a tracking generator coupled to a spectrum analyzer (HP89410A). The speaker and microphone are

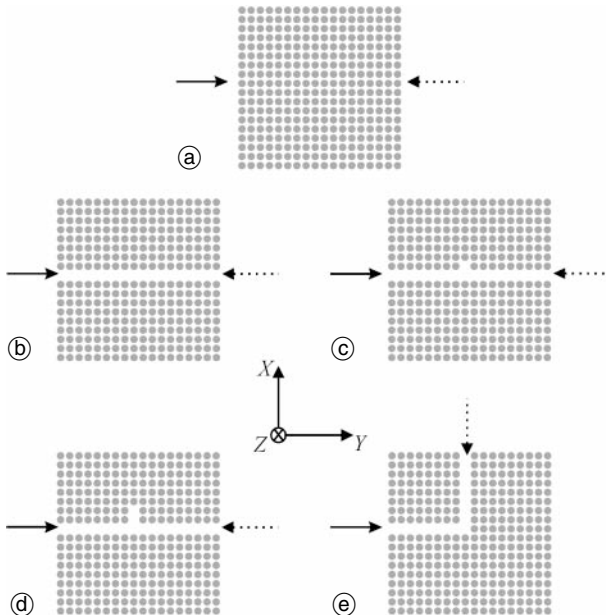


Fig. 1. Cross sections of the phononic crystals for the directions of propagation and the geometries considered in this paper. The PVC cylinders are parallel to the Z direction of the cartesian coordinate system $(OXYZ)$. The full and dashed arrows symbolize the location of the speaker and the microphone during the experimental process. (a) The IX direction of propagation along the perfect phononic crystal, (b) the perfect linear waveguide, (c) a stub of length equal to one period attached vertically to the waveguide, (d) a stub two periods long, and (e) a guide with a sharp bend.

placed against the walls of the structures in the same plane perpendicular to the cylinders. For each system, two measurements are conducted with and without the structure. The difference between these frequential signals is calculated to subtract any background effect.

2.2.2 Theoretical methods

a) PWE method: Band structures

In the most general case of wave propagation in a solid/solid periodic 2D inhomogeneous medium, one makes the assumption that the wave propagation is limited to the XY plane perpendicular to the cylinders. This has the effect of decoupling the elastic displacements in the XY plane (called XY or mixed-polarization modes) and those parallel to the Z direction denoted Z modes (transverse modes) [2, 3]. Since the 2D fluid/fluid phononic crystals can support only longitudinal acoustic waves, there is no need to decoupling the different modes and the problem of propagation in the composite is much simpler than for solids [15].

In the PWE method, the 2D periodicity in the XY plane allows one to develop the density and the elastic constants in Fourier series. Then, the equations of linear elasticity become standard eigenvalue equations for which the sizes of the matrices involved depends on the number of \mathbf{G} vectors of the reciprocal lattice taken into account in the Fourier series. The numerical resolution of the eigenvalue equations is performed along the principle directions of propagation of the 2D irreducible Brillouin zone of the array of inclusions (see inset of Fig. 2a). Numerical difficulties arise when considering mixed solid/fluid composites. While the equations of motion for solid/fluid composites are the same as for solid/solid systems, taking naively the transverse velocity of sound in the fluid equals to 0 results in convergence problems [16, 17]. To resolve this difficulty, we can make the solid part of the composite, rigid by assuming that its compressibility and its density are infinite. On the practical side, we replace the solid by a fluid with equivalent longitudinal speed of sound and density. In comparison to air, this solid is nearly rigid.

b) FDTD method: Transmission and band structures

The finite difference time domain method (FDTD) has been extensively used with success to study the propagation of electromagnetic waves through photonic band gap materials [17–19]. In recent years, this method has been extended to the investigation of acoustic wave propagation in inhomogeneous elastic media [12, 16, 17, 21, 22]. We apply the FDTD approach to calculate the transmission coefficients through finite thickness samples of phononic crystals and the dispersion curves of mixed solid/fluid composite materials. We limit the calculation to a strictly 2D FDTD scheme, that is the Z component of the elastic displacement, velocity, and stress fields are set equals to zero. In addition, we solve the 2D equations governing the motion inside the inhomogeneous medium in the XY plane. The Z dependency of any physical quantity is then neglected. The wave equation to be solved is

$$\rho(X, Y) \frac{\partial^2 \mathbf{u}}{\partial t^2} = \nabla \cdot \boldsymbol{\sigma} \quad (1)$$

where $\rho(X, Y)$ is the mass-density, \mathbf{u} and σ are the displacement field and the stress tensor. The component of the stress tensor are calculated from the elastic displacement using isotropic Hooke's laws with position dependent elastic coefficient $C_{11}(X, Y)$ and $C_{44}(X, Y)$. The latter elastic constant is zero for a fluid. To calculate the transmission coefficient of a finite size ABG composite, we construct a sample in three parts along the Y direction, a central region containing the finite phononic crystal sandwiched between two homogeneous regions. A travelling wave packet is launched in the first homogeneous part and propagates in the direction of increasing Y across the whole sample. Periodic boundary conditions are applied in the X direction perpendicular to the direction of propagation. Absorbing Mur's boundary [23] conditions are imposed at the free ends of the homogeneous regions along the Y direction. The incoming signal is a sinusoidal wave of pulsation ω_0 weighted by a Gaussian profile. In Fourier space this signal varies smoothly and weakly in the interval $[0, \omega_0]$. The input signal amplitude does not depend on X . Space and time are discretized with fine enough intervals to achieve convergence of the finite difference time domain algorithm. Further details concerning the numerical integration of the equation of motion can be found in Ref. [21]. The transmission spectrum along the ΓX direction of propagation in the irreducible Brillouin zone of the phononic crystal is calculated with an inhomogeneous region of thickness $18a$ along the Y direction and a width a along the X direction (i.e. 18 cylinders). For these structures the transmitted signal is averaged over the entire width of the system. A transmission coefficient is obtained by Fourier transforming the transmitted temporal signal and normalizing it to that of a homogeneous system composed of air. The central regions for the linear waveguide and the waveguides with a side branch resonator are constructed from a structure constituted of 18×18 periods. For this, cylinders are removed along the Y direction to form the guide and along the X direction to create the resonator. The signal exiting the guides is averaged over their width. The Fourier transform of the average exciting signal is again normalized to the Fourier transform of a signal propagating inside homogeneous air. In contrast to the case of the perfect phononic crystal, the normalization of the guided signal can give values of transmission exceeding 1 in linear scale or equivalently slightly positive values in dB.

To avoid difficulties encountered in the calculation of the band structure of mixed composites with the PWE method, Tanaka *et al.* [16] have reported an extension of the FDTD method for the calculation of dispersion relations of acoustic waves in 2D phononic crystals. In contrast with the standard FDTD approach, the band structure FDTD technique (BS-FDTD) implies a periodic system in the XY plane. The displacement field and the stress tensor must satisfy Bloch theorem

$$\mathbf{u}(\mathbf{r}, t) = e^{i\mathbf{K}\cdot\mathbf{r}} \mathbf{U}(\mathbf{r}, t), \quad (2)$$

$$\boldsymbol{\sigma}(\mathbf{r}, t) = e^{i\mathbf{K}\cdot\mathbf{r}} \boldsymbol{\Sigma}(\mathbf{r}, t) \quad (3)$$

where $\mathbf{r}(X, Y)$ is the position vector in the XY plane and $\mathbf{K}(K_X, K_Y)$ is the Bloch wave vector. $\mathbf{U}(\mathbf{r}, t)$ and $\boldsymbol{\Sigma}(\mathbf{r}, t)$ are

spatial periodic functions of period \mathbf{a} , the lattice translation vector. Inserting Eqs. (2) and (3) into (1) as well as in Hooke's law results in equations of motion for \mathbf{U} . To solve them, one first specifies a 2D wave vector, \mathbf{K} , along the principal direction of the irreducible Brillouin zone. An assumption on the initial displacement $\mathbf{U}(\mathbf{r}, t=0)$ in the form of a delta stimulus at some random location within the unit cell is then made. The equations of motion are solved by discretizing both space and time. The time evolution of $\mathbf{U}(\mathbf{r}_i, t)$ at several predetermined locations within the unit cell is recorded. Peaks in the frequency space of the Fourier-transformed signals are identified as the eigen frequencies of the normal modes of the system for the wave vector, \mathbf{K} . In contrast to the PWE method, the band structure FDTD technique allows us to compute the band structure of periodic mixed solid/fluid composite materials without requiring the assumption of solid rigidity.

The physical parameters used in these calculations are the longitudinal, C_l , transverse, C_t , speeds of sound and the mass density, ρ for the solid. The acoustic properties of a fluid like air are the longitudinal speed of sound and the density. For all calculations we use $C_l = 2230$ m/s, $C_t = 1000$ m/s and $\rho = 1364$ kg/m³ for PVC, and $C_l = 340$ m/s and $\rho = 1.3 \times 10^{-3}$ kg/m³ for air.

3. Results

3.1 Perfect phononic crystal

Figure 2a presents the band structures along the ΓX direction of propagation computed with both the PWE and the FDTD methods. The PWE band structure was calculated with 169 \mathbf{G} vectors of the reciprocal space. In the range of frequency of Fig. 2a, there exists a large stop band between 2.8 and 10 kHz. The very good agreement between the two theoretical methods validates the assumption of the rigidity of the solid in the peculiar case of the PVC/air composite in this range of frequency. Figures 2b and 2c show the experimental and theoretical transmission spectra of the PVC/air phononic crystal along the ΓX direction of propagation, respectively. The measured transmission is drastically depressed in the interval of frequency [3, 10] kHz. This stop band is also confirmed by the computed transmission and agrees with the band structure calculations. On the other hand, we have verified experimentally and theoretically via PWE and FDTD calculations, that along the ΓM direction, a stop band extends from 4 to 10 kHz. This shows that the PVC/air phononic crystal possesses an **absolute** band gap in the audible frequency range between 4 and 10 kHz. This interval of frequency is the intersection of the gaps in the ΓX and ΓM directions.

3.2 Linear waveguide

In this section, we investigate the properties of a 2D phononic crystal made of PVC cylinders surrounded by air and containing a straight wave guide (see Fig. 1b). Figure 3a reports its band structure. These dispersion curves were obtained numerically, on one hand, using the PWE method (solid lines) with a supercell of 7 periods. The super-

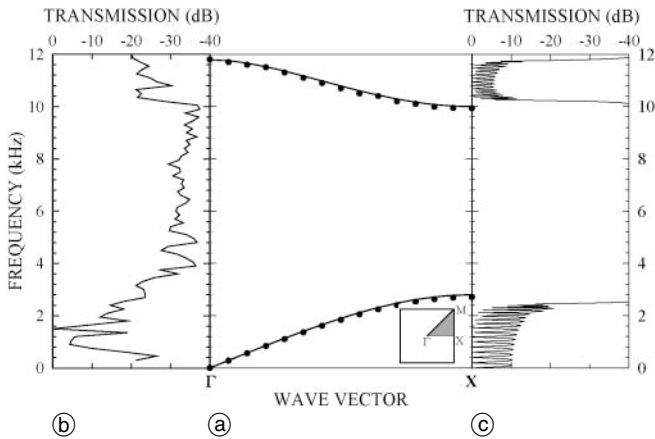


Fig. 2. (a) Band structures of the perfect PVC/air phononic crystal along the ΓX direction of propagation of the irreducible Brillouin zone (see inset) computed with the PWE (solid lines) and the FDTD (dots) methods. Experimental (b) and theoretical (c) transmission coefficients along the ΓX direction.

cell contains 7 unit cells, one of which is filled with air only. The supercell is also repeated periodically in the X direction leading to a stack of waveguides separated by 7 periods in this direction. This separation is sufficient to avoid coupling between neighboring guides. The PWE band structure was calculated with 1105 \mathbf{G} vectors. On the other hand, the band structure was also computed with the help of the FDTD method (dots) and the agreement with the PWE calculations is again quite good. The slight difference in frequency of the FDTD bands compared to those obtained with the PWE method results from the fact that the PWE calculation has not fully converged with respect to the \mathbf{G} vectors [16]. The dispersion curves numbered 6, 7, 8 and 9 are related to localized modes in the straight waveguide. The measured and calculated transmission spectra of the linear waveguide are presented in Figs. 3b and 3c, respectively. Experimentally, the waveguide permits transmission of waves that otherwise would be forbidden in the perfect phononic crystal. There are two

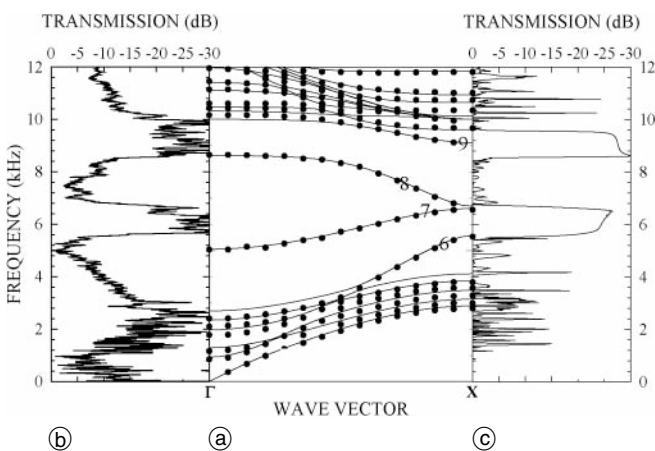


Fig. 3. (a) PWE (solid lines) and FDTD (dots) band structures of a PVC/air phononic crystal containing a straight waveguide along the Y direction (see Fig. 1b). The supercell contains 1×7 unit cells. Experimental (b) and theoretical (c) transmission spectra along the linear waveguide. The bands numbered 6, 7, 8 and 9 in Fig. 3a are associated with waveguides modes. Bands 7 and 9 are “deaf bands” and do not contribute to the transmission (see text for details).

waveguide passing bands with frequency intervals [2.4, 5.6] kHz and [6.8, 8.5] kHz. Transmission of waves with frequency in these intervals takes place along the waveguide without any loss. Stops bands still exist for frequencies between 5.6 and 6.8 kHz and 8.5 and 10 kHz. The experimental spectrum is confirmed by the FDTD calculation. Indeed the right panel of Fig. 3 shows two passing bands from 0 to 5.5 kHz and 6.8 to 8.5 kHz, separated by a region with low transmission that extends from 5.5 to 6.8 kHz. The gap of the perfect phononic crystal persists for frequencies in the range [8.5, 9.6] kHz.

A comparison between the transmission spectra and the band structures indicates that the dispersion curves labeled 7 and 9 in Fig. 3a do not contribute to the transmission. An analysis of the symmetry of these modes may explain this singular effect. For this, using the PWE method, we compute some eigenvectors associated with the bands 6 through 9 at a given wave vector. The Fourier transform of the eigenvectors yields the pressure field inside the phononic crystal [11]. Figure 4 illustrates the pressure field pattern corresponding to the 6th, 7th, 8th and 9th bands at the X point of the irreducible Brillouin zone. It is important to note that the 6th and 8th modes have a symmetry readily excitable by an incident wave of longitudinal polarization. In contrast, the 7th and 9th modes are anti-symmetric with respect to the symmetric plane of the waveguide. Consequently, these antisymmetric modes cannot be

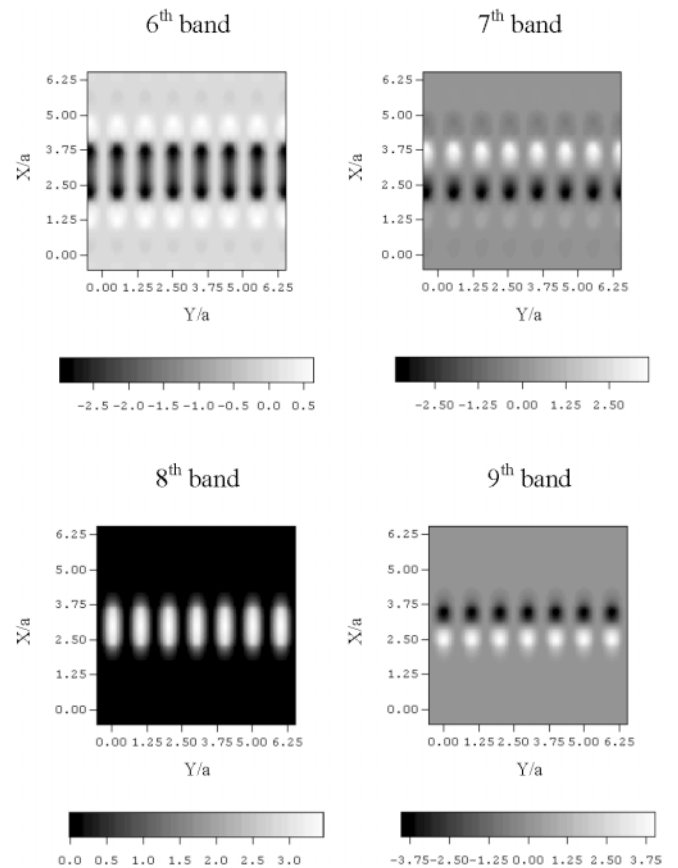


Fig. 4. Pressure fields inside the PVC/air phononic crystal containing a straight waveguide. The grey scale indicates the relative amplitude of the pressure field. These maps were obtained from the PWE computations of the eigenvectors associated with the 6th, 7th, 8th and 9th eigenfrequencies at the X point of the irreducible Brillouin zone (see Fig. 3a).

excited by a longitudinal incident wave and will not contribute to the transmission. Modes of this kind, named “deaf bands”, were reported for perfect photonic or phononic crystals [11, 24–27]. Let us stress again that the deaf modes reported in this paper are not modes of the perfect crystals but waveguide modes.

In Fig. 4, the centers of the cylinders in the phononic crystal are located at integer values of the ratios X/a and Y/a , excluding $X/a = 3$ which is the position of the symmetry plane of the waveguide. The rigidity of the inclusions explains that the acoustic waves do not penetrate inside the cylinders and this leads to a vanishing pressure field inside the inclusions. The air waveguide is bound by PVC cylinders at $X/a = 2 + r/a = 2.48$ and $X/a = 4 - r/a = 3.52$, that is, its width is equal to $1.04a$. The acoustic pressure field extends significantly beyond these bounds, showing that the waveguide modes are not strictly confined inside the waveguide. At larger distances from the waveguide boundaries, the pressure field vanishes everywhere since the frequency of the propagating waves falls inside the stop band of the perfect phononic crystal. In a previous study of a waveguide in air/water and steel/water 2D phononic crystals, the guiding modes were shown to obey classical waveguide models with strictly perfectly reflecting walls [4]. The extent of the pressure field outside the limits of the waveguide in the PVC/air system indicates that in this particular case the waveguide modes can not be derived analytically from simple waveguide theory. It therefore appears that straightforward and generalized application of this theory to waveguides in phononic crystals can be misleading.

3.3 Linear waveguides with side branch resonator

The effect of a side branch resonator on the transmission spectrum of the waveguide is illustrated in Figs. 5 and 6. The removal of a single cylinder adjacent to the waveguide produces a resonator of nominal length a . The calculated transmission spectrum in Fig. 5a retains the general characteristics of the linear waveguide (see Fig. 3c) with two additional features. Narrow dips appear in the calculated transmission spectrum at two frequencies, namely 4.7 and 7.5 kHz. These reductions in transmission are similar in nature to those observed in a recent theoretical study of waveguides with side branch resonators in water/air and steel/water phononic crystals [4]. The transmission in the waveguide is significantly altered due to interference phenomena between the acoustic modes of the guide and those of the resonator. The characteristics of the experimental spectrum of the guide with resonator of length a are best seen by calculating the difference between the transmission along the guide with resonator and that of the perfect linear guide as reported in the insets of Fig. 5b. A small depression in transmission occurs in the first passing band of the linear guide at 4.85 kHz. This agrees quite well with the theoretically predicted dip at 4.7 kHz (see Fig. 5a). In the range [7, 8.5] kHz, the experimental transmission spectrum exhibits two depressions around 7.5 kHz and 8.2 kHz. Since the first depression is in accordance with the one observed in the theoretical transmission, the feature at 8.2 kHz have no analog in Fig. 5a. Nevertheless,

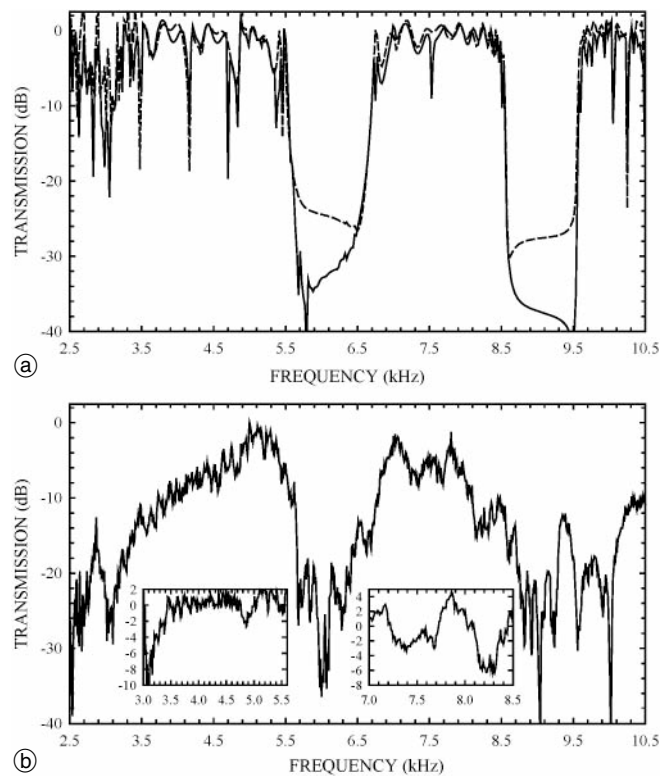


Fig. 5. Theoretical (a) and experimental (b) transmission spectra along the linear waveguide with a side branch of nominal length a . The insets represent the difference between the transmission in the guide with resonator and the transmission in the linear waveguide in the range of frequency associated with the passing bands of the linear guide. The dashed line in Fig. 5a represents the computed transmission along the linear waveguide of Fig. 3c.

one notes that this feature appears in the very near vicinity of the edge of the second waveguide passing band and this renders its analysis very difficult.

Lengthening the resonator increases the number of resonant modes and therefore the number of narrow dips in the transmission spectrum of the guide with resonator. For instance, in the case of Fig. 6a where the resonator is twice as long as in Fig. 5, the theoretical transmission spectrum exhibits four narrow dips in transmission at 3.95, 7.3, 9.7 and 9.8 kHz. The experimental spectrum of the guide with a resonator of length $2a$ possesses a significant reduction in transmission at 4.1 kHz in very good agreement with the first calculated dip (see Fig. 6a). Two additional and well-defined depressions in transmission are observed in the second passing band of the guide at the frequencies 7.4 and 8.2 kHz. As in the previous case, the first of these two features is in good agreement with the theoretical predictions but the second one which appears in the near vicinity of the stop band has no equivalent in Fig. 6a. Because the second stop band in the experimental spectrum (see Fig. 3) is larger than the theoretically predicted transmission band gap, the dips calculated around 9 kHz cannot be observed experimentally.

A comparison between Figs. 5b and 6b reveals that the influence of the resonator on the waveguide transmission is much more pronounced with a longer resonator. For instance, the first depression in transmission which occurs around 4.5 kHz in these two figures is much more important with a resonator of nominal length $2a$ than a . As

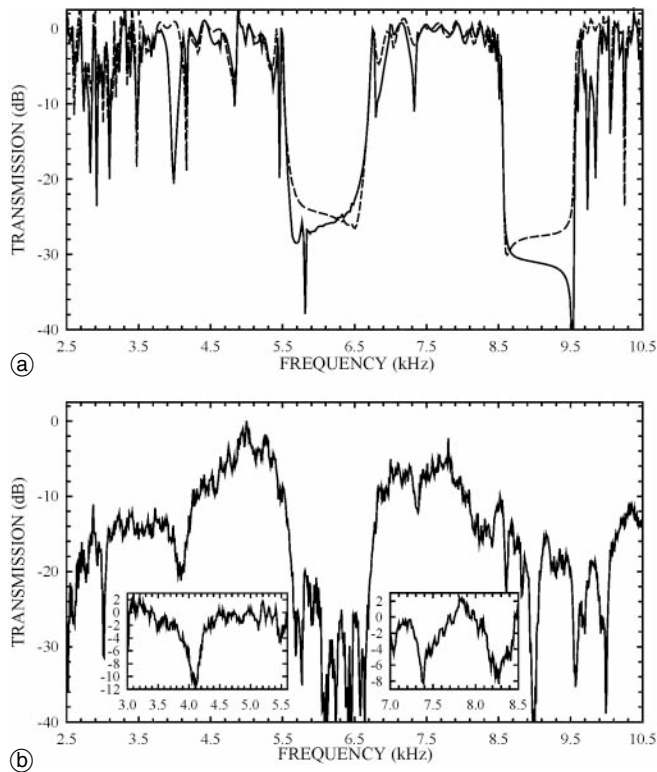


Fig. 6. Theoretical (a) and experimental (b) transmission spectra along the linear waveguide with a side branch of nominal length $2a$. The insets represent the difference between the transmission in the guide with resonator and the transmission in the linear waveguide in the range of frequency associated with the passing bands of the linear guide. The dashed line in Fig. 6a represents the computed transmission along the linear waveguide of Fig. 3c.

noted before, the waveguide modes extend significantly beyond the physical bounds of the guide. The interference between these modes and those of a short resonator are therefore anticipated to be weak. Simple models based on one-dimensional waveguides coupled to one-dimensional resonators introduced in [4] will not be applicable to systems such as those studied here where the guiding modes are not strictly confined inside the bounds of the guide.

3.4 Bent waveguide

The transmission spectrum along a bent waveguide (Fig. 7) is similar to that of the linear guide. This spectrum is measured by emitting sound waves at the entrance of the guide and collecting the signal at its exit. This result demonstrates that acoustic waves can be transmitted without significant loss along a guide with sharp bends. To verify that transmission occurs without much loss, we have also measured the transmission by placing the speaker at the entrance of the bent guide and the microphone on the opposite side. In this case one recovers the transmission spectrum in the IX direction of the perfect phononic crystal. The most significant difference between the transmission spectra of the linear and bent waveguide arises in the form of dips in the passing bands of the latter. The most notable features occur at 4.5 kHz and 7.3 kHz and are reminiscent of the dips in the transmission spectrum of a guide with a side branch resonator of nominal length $2a$. The observed features appear therefore

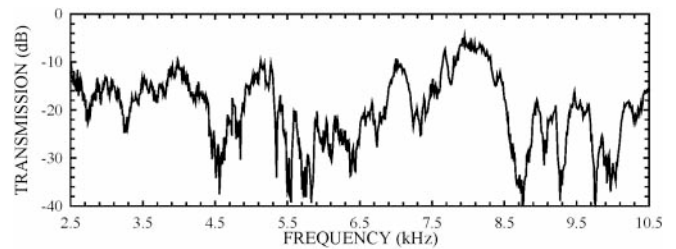


Fig. 7. Experimental transmission spectrum for propagation along the bent waveguide.

to be due to interferences between the incident wave and waves reflected by the bend.

4. Conclusions

The experimental results presented in this paper report primarily on the transmission of audible acoustic waves along waveguides in a two-dimensional phononic crystal. We show the existence of deaf modes in the band structure of the waveguide. We demonstrate the possibility of resonant filtering in a linear phononic crystal waveguide with one single side branch resonator. Frequency filtering takes place by reduction of the transmission at specific frequencies within the passing band of the waveguide. These frequencies depend on the length of the resonator. The experimental results are in fair agreement with theoretical calculations based on the FDTD method, especially at the lowest frequencies studied. A waveguide with a sharp bend appears to transmit acoustic waves without significant loss over most of the passing band of a linear guide. Similarly to the linear guide with resonator, transmission along the bent waveguide is significantly reduced at some specific frequencies which is believed to be due to interference between incident and reflected waves near the bend. The structures presented in this paper may serve as element in the design of devices for the treatment of acoustic signals such as filtering or demultiplexing.

Acknowledgments. The authors acknowledge “Le Fond Européen de Développement Régional” (FEDER) and “Le Conseil Régional Nord-Pas de Calais” for providing part of the computer facilities.

One of us (B.D.R.) would like to thank Dr. A. Khelif for helpful discussions.

References

- [1] Sigalas, M. M.; Economou, E. N.: Band structure of elastic waves in two dimensional systems. *Solid State Commun.* **86** (1993) 141–143.
- [2] Kushwaha, M. S.; Halevi, P.; Dobrzynski, L.; Djafari-Rouhani, B.: Acoustic band structure of periodic elastic composites. *Phys. Rev. Lett.* **71** (1993) 2022–2025.
- [3] Vasseur, J. O.; Djafari-Rouhani, B.; Dobrzynski, L.; Kushwaha, M. S.; Halevi, P.: Complete acoustic band-gaps in periodic fibre reinforced composite materials: the carbon/epoxy composite and some metallic systems. *J. Phys.: Condens. Matter.* **6** (1994) 8759–8770.
- [4] Khelif, A.; Djafari-Rouhani, B.; Vasseur, J. O.; Deymier, P. A.; Lambin, Ph.; Dobrzynski, L.: Transmittivity through straight and stublike waveguides in a two-dimensional phononic crystal. *Phys. Rev. B* **65** (2002) 174308.

- [5] Kafesaki, M.; Sigalas, M. M.; Garcia, N.: Frequency modulation in the transmittivity of wave guides in elastic-wave band-gap Materials. *Phys. Rev. Lett.* **85** (2000) 4044–4047.
- [6] Miyashita, T.; Inoue, C.: Numerical investigations of transmission and waveguide properties of sonic crystals by finite-difference time-domain method. *Jpn. J. Appl. Phys.* **40** (2001) 3488–3492.
- [7] Khelif, A.; Djafari-Rouhani, B.; Vasseur, J. O.; Deymier, P. A.: Transmission and dispersion relations of waveguide structures in phononic band gap materials. *Phys. Rev.* **B68** (2003) 024302.
- [8] Chandra, H.; Deymier, P. A.; Vasseur, J. O.: Elastic wave propagation along waveguides in three dimensional phononic crystals. *Phys. Rev.* **B70** (2004) 054302.
- [9] Torres, M.; Montero de Espinosa, F. R.; Garcia-Pablos D.; Garcia, N.: Sonic band gaps in finite elastic media: Surface states and localization phenomena in linear and point defects. *Phys. Rev. Lett.* **82** (1999) 3054–3057.
- [10] Montero de Espinosa, F. R.; Jimenez, E.; Torres, M.: Ultrasonic band gap in a periodic two-dimensional composite. *Phys. Rev. Lett.* **80** (1998) 1208–1211.
- [11] Sanchez-Perez, J. V.; Caballero, D.; Martinez-Sala, R.; Rubio, C.; Sanchez-Dehesa, J.; Meseguer, F.; Llinares, J.; Galves, F.: Sound attenuation by a two-dimensional array of rigid cylinders. *Phys. Rev. Lett.* **80** (1998) 5325–5328.
- [12] Vasseur, J. O.; Deymier, P. A.; Chenni, B.; Djafari-Rouhani, B.; Dobrzynski, L.; Prevost, D.: Experimental and theoretical evidence for the existence of absolute acoustic band gaps in two-dimensional solid phononic crystals. *Phys. Rev. Lett.* **86** (2001) 3012–3015.
- [13] Miyashita, T.; Inoue, C.; Sakata, K.: Full band-gap of sonic crystals composed of a periodic array of acrylic cylinders in air – Numerical predictions and experimental observations – Poster session on “Numerical methods in acoustics” – 17th International Congress on Acoustics (Rome, September 2–7, 2001).
- [14] Khelif, A.; Choujaa, A.; Benchabane, S.; Djafari-Rouhani, B.; Laude, V.: Guiding and bending of acoustic waves in highly confined phononic crystal waveguides, *App. Phys. Lett.* **84** (2004) 4400–4402.
- [15] Vasseur, J. O.; Djafari-Rouhani, B.; Dobrzynski, L.; Deymier, P. A.: Acoustic band gaps in a two-dimensional Boron-Nitride like structure. *J. Phys.: Condens. Matter* **9** (1997) 7327–7341.
- [16] Tanaka, Y.; Tomoyasu, Y.; Tamura, S.: Band structure of acoustic waves in phononic lattices: Two-dimensional composites with large acoustic mismatch. *Phys. Rev.* **B62** (2000) 7387–7392.
- [17] Garcia-Pablos, D.; Sigalas, M.; Montero de Espinosa, F. R.; Torres, M.; Kafesaki, M.; Garcia, N.: Theory and experiments on elastic band gaps. *Phys. Rev. Lett.* **84** (2000) 4349–4352.
- [18] Taflove, A.: *The Finite Difference Time Domain Method*. Artech, Boston, 1998.
- [19] Chan, C. T.; Yu, Q. L.; Ho, K. M.: Order-N spectral method for electromagnetic waves. *Phys. Rev.* **B51** (1995) 16635–16642.
- [20] Fan S.; Villeneuve, P. R.; Joannopoulos, J. D.: Large omnidirectional band gaps in metallodielectric photonic crystals. *Phys. Rev.* **B54** (1996) 11245–11251.
- [21] Lambin, Ph.; Khelif, A.; Vasseur, J. O.; Dobrzynski, L.; Djafari-Rouhani, B.: Stopping of acoustic waves by sonic polymer/fluid composites. *Phys. Rev.* **E63** (2001) 066605.
- [22] Sigalas, M. M.; Garcia, N.: Theoretical study of three dimensional elastic band gaps with the finite-difference time-domain method. *J. Appl. Phys.* **87** (2000) 3122–3125.
- [23] Mur, G.: Absorbing boundary conditions for the finite-difference approximation of the time-domain electro-magnetic field equations. *IEEE Trans. Electromagn. Comput.* **23** (1981) 377–382.
- [24] Robertson, W. M.; Arjavalingam, G.; Meade, R. D.; Brommer, K. D.; Rappe, A. M.; Joannopoulos, J. D.: Measurement of photonic band structure in a two-dimensional periodic dielectric array. *Phys. Rev. Lett.* **68** (1992) 2023–2026.
- [25] Krauss, T. F.; de la Rue R. M.; Brand, S.: Two-dimensional photonic-bandgap structures operating at near-infrared wavelengths. *Nature (London)* **383** (1996) 699–702.
- [26] Karathanos, V.: Inactive frequency bands in photonic crystals. *J. Mod. Opt.* **45** (1998) 1751–1758.
- [27] Psarobas, I. E.; Modinos, A.; Sainidou, R.; Stefanou, N.: Acoustic properties of colloidal crystals. *Phys. Rev.* **B65** (2002) 064307.